

PACS numbers: 71.36.+c, 72.80.Vp, 73.20.Mf, 81.05.ue, 84.40.Az, 84.40.Ba, 85.35.-p

Inter/Intra-Chip Optical Wireless Communication with Robust Plasmonic Nanoantenna Design

T. R. Sangeeta and J. Deny

*Department of Electronics and Communication Engineering,
Kalasalingam Academy of Research and Education,
626126 Krishnankoil, Virudhunagar District, Tamilnadu, India*

This research aims to improve antenna efficiency in inter/intra-chip optical wireless communication by utilizing plasmonic materials. The proposed model uses an AgSi ground plane with a silver-coated silicon cube, which mitigates interband transition, while enhancing plasmonic resonance. A planar plasmonic substrate with atomic MoS₂ on a silver surface acts as a barrier against unwanted molecule infiltration, preventing interband transition. A novel bi-rhombic hybrid nanostrip waveguide is introduced, featuring two parallel rhombic layers with a hybrid Ag–silicon ribbon material to mitigate ohmic losses and enhance propagation. The rhombic configuration reduces ohmic losses and optimally amplifies light intensity. The antenna performance is simulated and evaluated using ANSYS HFSS 2019 R3 software, revealing superior performance compared to conventional models, validating its efficacy in inter/intra-chip optical wireless communication applications.

Це дослідження спрямовано на підвищення ефективності антени в оптичному бездротовому зв'язку між чіпами та всередині чіпу шляхом використання плазмонних матеріалів. Запропонований модель використовує заземлену площину AgSi із кремнійовим кубом, покритим сріблом, який пом'якшує міжзонний перехід, одночасно посилюючи плазмонний резонанс. Пласка плазмонна підкладка з атомарним MoS₂ на поверхні срібла діє як бар'єр проти небажаної інфільтрації молекул, запобігаючи міжзонним переходам. Представлено новий біромбічний гібридний наносмушковий хвилевід, який містить два паралельні ромбічні шари з гібридним матеріалом стрічки Ag–кремній для зменшення омичних втрат і посилення поширення. Ромбічна конфігурація зменшує омичні втрати й оптимально підсилює інтенсивність світла. Ефективність антени моделюється й оцінюється за допомогою програмного забезпечення ANSYS HFSS 2019 R3, що показує ліпшу продуктивність порівняно зі звичайними моделями, підтверджуючи її ефективність у застосуваннях оптичного бездротового зв'язку між чіпами.

Key words: plasmonic material, bi-rhombic structure, nanostrip waveguide, MoS₂ layer, ANSYS HFSS, inter/intra-chip optical wireless communication.

Ключові слова: плазмонний матеріал, біромбічна структура, наностричковий хвилевід, шар MoS₂, ANSYS HFSS, між/внутрішньочіповий оптичний бездротовий зв'язок.

(Received 12 September, 2023; in revised form, 27 October, 2023)

1. INTRODUCTION

Wireless communications largely depend on the extensive applications of antenna designs for microwave and radio wave frequencies. Optical nanoantennas are less common than traditional antennas because of their small size. Nevertheless, recently, nanotechnology and manufacturing advancements have enabled the construction of frameworks as small as nanometres paving the way for new and improved optical nanoantenna designs [1]. Nowadays nanosize optical antennas have been proposed for a variety of tasks in the near-infrared, far-infrared, and visible ranges. Nanoantennas were already recognized as active and auspicious components in the fields of sprinkling [2, 3], ability to sense [4, 5], photodetection [6, 7], thermal expansion [8, 9], inter- and/or intra-chip optical communications [10, 11], and many others. Additionally, an optical nanoantenna can be extremely helpful in lowering energy usage and enabling faster on-chip optical communication. It is also regarded as a viable option for photonic waveguide-based connectors for on-chip Wi-Fi transfer with significant spectral efficiency [8].

Because of the emergence of uses in professional fields such as augmented/virtual reality, machine learning, vehicle connectivity, and cloud systems, high computing complexity is currently in demand [9]. Trends in calculation procedures are thus encouraging the development of Chip Multicore Processors as well as Strong Performance Computing designs, in which various components are merged to meet the demand for ongoing performance growth. The communication losses, which occur in wired connections, can be greatly reduced by using optical wireless nanolinks with nanoantennas [10].

Wireless Network on Chip in optical communication is being studied as a potential solution to the physical interconnection bottleneck. Optical wireless networks-on-chip had also been studied recently to maintain the major benefits of a Wireless Network On-Chip with short delay as well as simplified network planning while relieving the antenna reform process. This is due to obvious issues

with on-chip assimilation in millimetre-wave antennas [11]. Because wireless network-on-chip is intended to supplement instead of removing connected remedies, they gain from entire interoperability with optical, network servers that can be placed on a similar processor. The design entails several difficult challenges, ranging from wireless channel modelling and optical antenna design to management and avoidance of interfering problems, which invariably arise because the wireless transmission channel is shared by multiple simultaneous wireless infrastructures [12].

Some research scenarios based on various antenna configurations that improve performance are used to analyse the transmission and effectiveness of the wireless associations in optical wireless networks-on-chip. One of its important design components is the antenna that is attached to the optical waveguide since it enables switching from wireless to wired visual transmission and vice versa [13]. The optical signal from the input waveguide is radiated by the antenna at the receiving section into the surrounding medium. The transceiver then transmits the wirelessly propagating signal to an output waveguide [14]. The communication efficiency is not performing well, despite the impressive study results for wireless optical nanoconnections. Therefore, additional research is required to remove this restriction [15].

The photoconductive terahertz source has far better efficiency than terahertz sources made on short-carrier-lifetime substrates. The tight three-dimensional confinement of the optical pump beam around the terahertz nanoantennas used as radiating elements is the source's most novel characteristic. This is accomplished by forming a nanocavity with plasmonic structures and a dispersed Bragg reflector [16]. As a result, a very high, ultrafast current is generated, which drives the nanoantennas to produce broadband terahertz radiation. Experiment shows that this terahertz generator can create 4-mW pulsed terahertz radiation over the 0.1–4-THz frequency band with an optical pump output of 720 mW. This is the highest reported power level for terahertz radiation from a photoconductive terahertz source, representing an order of magnitude improvement in optical-to-terahertz conversion efficiency over state-of-the-art photoconductive terahertz sources fabricated on short carrier-lifetime substrates.

The design, optimization, and manufacturing of a plasmon-assisted terahertz (THz) photoconductive antenna (PCA) for THz pulse generation at low-power optical pumps are described in this paper [17]. In the photoconductive gap, a high aspect-ratio dielectric-embedded plasmonic Au grating is embedded. Moreover, the photoconductor Si_3N_4 passivation and the Al_2O_3 antireflection coating are used to improve antenna performance. These findings show

that the plasmonic PCA has a high potential for use with low-power lasers, paving the way for the creation of portable and cost-effective THz spectrometers and imaging devices.

This study offers a dependable plasmonic material-based technique for optical wireless nanoantennas that addresses the difficulties of terahertz signal propagation beyond a few meters. Various materials, topologies, frequencies, and qualities affect surface plasmon propagation, and precious metals exhibit considerable optical loss as a result of interband transitions. Improved information security, lower power losses, higher plasmonic properties, and less interference with optical-system components are all dependent on decreasing side lobes.

In this study, we introduce a novel method where the geometrical, structural, and material properties were enhanced for improving the directivity and high sensitivity of nanoscale optical wireless communication to achieve communication efficiency that is higher than prior methods, even across ultra-long variations. The following is a description of this research's primary goals:

the planar plasmonic substrate is designed with MoS_2 to limit interband transmission, and the AgSi ground plane is constructed using silver-coated silicon cubes, which tend to reduce interband transition and improve plasmonic resonance;

to reduce ohmic losses and improve propagation, a novel bi-rhombic hybrid nanostrip waveguide has been modelled with two parallel rhombic layers using a hybrid material of Ag with silicon ribbon;

additionally, a graphite spherical resonator is used, where the spherical structure suppresses the side lobe due to its high efficiency, thermal stability, and radiating properties.

As a result, our work outperforms all current methods, and the remaining component of this research includes. The literature review for this research is defined in Section 2, and the proposed technique and its features are described in Section 3. Part 4 summarises the findings and discusses our novel approach. Part 5 concludes our discussion.

2. LITERATURE SURVEY

Using a unified mathematical framework, Nafari *et al.* [16] reviewed and compared magnetic plasmonic nanoantennas for the optical wireless transmitter. This framework takes into account the metal's properties, such as complex problem conductivity and transmittance, the propagation features of plasmon resonance polariton signals on the nanoantenna, such as confinement component as well as transmission duration, and the transmitter geometrical, such as size as well as diameter. The framework enables the analyti-

cal calculation of the produced plasmonic power supply during the reception, as well as the total emitted strength and transmission performance. The support surface plasmon polaritons (SPP) wave confinement component has been shown experimentally and numerically to have a significant effect on the bandwidth and efficiency of nanoantennas in this study. However, the antenna effectiveness was decreased by a significant interband transition.

With 6G applications at 474 THz, Alves *et al.* [17] offered a technological solution for extremely long intra/inter-chip optical wireless. Nanoconnections are created by combining two distinct nanoantennas, horn and planar antenna. Four different horn and planar antenna configurations were tested to pick the optimum setup for broadening the system's capabilities. According to numerical simulations, the optical emitters, as well as receivers, are correctly planned to offer reduced optical-transmission losses, low replication coefficient points, great directivity, and great gain, resulting in an ultra-long intra/inter-chip optical wireless nanolink of 32 and 40 dB advancement in the link budget. However, spreading loss and absorption in the medium decreased the light-beam intensity.

The presentation by Ahmad *et al.* [18] of a broadband optical nanoantenna with a profit of up to 11.4 dBi (dBi \equiv dB(isotropic)) for a monocomponent transmitter in nanophotonic functionalities will include a broader variety of optical transmission frequencies (666 to 6000 nm). The proposed antenna-distinguishing feature is a hybrid plasmonic waveguide-based feed that accepts the optical power from the planar waveguide as well as directs it away from the plane. As a result, the proposed antenna has highly directional radiation properties, making it an excellent candidate for inter- and intra-chip optical communications and sensing. To increase yield and directionality, the work was expanded to an array configuration of order 2×1 and 64×1 . To get a decent propagation length, the side lobe might be reduced further.

According to Biswas *et al.* [19], a modified bowtie plasmonic nanoantenna based on graphene could have periodic directors produced by slots above the radiating structure that resonate in the optical frequency range. Only several optical nanosensors for constructing multipath wireless nanorelationships have been mentioned in the field of nanophotonics. The highest absorption power of the graphene sheet resulted in the greatest directivity of 9.67 dBi at the telecommunication frequency of 1550 nm by selecting the chemical potential of 0.5 eV (193.5 THz). A dynamically monitored triple-directional radioactivity beam was produced using the proposed graphene-based slotted bowtie optical nanotransmitter. Combining a collection of our recommended optical metamaterials nanoantennas with this special nature allows for a multipath intra- or inter-on-

chip Wi-Fi nanorelationship for secure optical file transfers. However, it is still necessary to reduce surface plasmon propagation losses.

A switched-beam nanoantenna for the THz wave domain was demonstrated by Dash *et al.* [20]. Based on the Yagi–Uda antenna architecture, this study presented switched-beam graphene nanoantennas on silicon dioxide (SiO_2) substrates. Antenna-I in one scenario can only switch the beam in a 90° direction, whereas Antenna-II in the other scenario can do so in a 0° , 90° , and 180° directions. By modifying graphene conductivity through its chemical potential, reconfigurability is made possible. The planned graphene nanoantenna resonates at a sub-wavelength scale due to the plasmonic direction of propagation in nanomaterials at THz. The nanoantenna is both pattern and frequency reconfigurable, as evidenced by the pat-

TABLE. Systematic survey.

Ref. No.	Author	Techniques	Significance	Limitation
16	Monanafari	In this study, metallic plasmonic nanoantennas for wireless optical communication are modelled and examined	High bandwidth for data transmission	Limited range compared to other wireless technologies
17	A. A. C. Alves	In this study, an effective technological approach for an extremely long intra/inter-chip optical wireless nanolink is presented. It is based on the cooperative usage of two distinct nanoantennas, the horn and plantenna, with 6G applications targeted at 474 THz	Due to the activation of localized surface plasmon resonances in the plantenna, the power link budget was increased by 40 dB when a horn nanoantenna, an optical emitter with strong directivity, was used in conjunction with an optical receiver	Researchers suggest creating plasmonic nanoantennas using femtosecond direct laser writing lithography for use in intra/inter-chip optical wireless nanolinks as future work
18	Inzamam Ahmad	This article introduces a broadband optical nanoantenna for nanophotonic applications that covers a wider range of optical communication wavelengths (666 to 6000 nm)	Substantial gain of up to 26.8 dBi	Transmission can be disrupted by moving objects

Continuation TABLE.

Ref. No.	Author	Techniques	Significance	Limitation
19	Richard Victor Biswas	This work proposes a modified bowtie plasmonic nanoantenna based on graphene that resonates throughout the optical frequency spectrum with the periodic directors produced by the slots on top of the radiating structure	Due to the graphene sheet's highest absorption capacity, the maximum directivity of 9.67 dBi has been achieved	Limited penetration through walls and solid objects
20	Sasmita Dash	The switched-beam nanoantenna for the THz wave area is presented in this research	Complex alignment required for optimal performance	Alignment and setup can be time-consuming

tern reconfigurability that may be detected over a broad frequency series. Additionally, the antenna workability may have been improved by using low-loss plasmonic material.

Kavitha *et al.* [21] built and examined plasmonic nanopatch antennas on graphene. The chemical potential of graphene was utilized to alter the Kubo conductivity formula, which was used to determine the conductivity of graphene. Furthermore, the Drude dispersive model of graphene exhibits negative real permittivity, which is required for plasmonic resonance. The created graphene nanopatch antenna is ideal for terahertz transmission, with a gain of 3.52 dB at 30 THz. By differing the chemical reactivity, it is illustrated that the graphene nanoantenna array resounds at a range of frequencies, with three resonating frequencies of 30, 115, and 176 THz being recorded at 1.3 eV chemical potential with adequate features. By modifying the square geometry of the graphene nanoantenna array to an *L*-shape, the antenna gain is nearly tripled. Still, the bending direction of propagation is a problem that needs to be taken into account.

As a result, in Ref. [16], there was a significant interband change, which decreased antenna efficiency. In Ref. [17], expanding failure and assimilation in the media reduced the intensity of the light beam. To get a decent propagation length, the side lobe can be attenuated more [18]. However, the losses in surface plasmon propagation must be reduced [19]. To improve the antenna viability, low-loss plasmonic material may have been employed [20]. The bend-

ing direction of propagation is a problem in Ref. [21] that needs to be taken into account. A unique micro transmitter must be built to achieve effective inter/intra-chip wireless optical interaction.

3. PROPOSED METHODOLOGY

In large-distance optical wireless communication, beyond a few meters, propagation becomes challenging for terahertz (THz) signals because of high spreading loss and absorption. Thus, there is a need to develop a new model, which is highly efficient in transmitting the information without many losses and propagates the signal to the wide bandwidth and thereby increasing the nanoantenna radiation efficiency, which can be used for inter/intra-chip optical wireless communication. This research proposes to utilize plasmonic material to improvise the antenna efficiency. The conventional nanoantenna utilized plasmonic metals such as gold and silver, but still, they exhibit certain optical loss due to the interband transitions leading to high spreading loss and absorption in the media causing low antenna radiation efficiency. This research overcomes the interband transition issue by utilizing a distinctive material combination with the AgSi ground plane, which is made up of a silver-coated silicon cube. The silicon coating tends to mitigate the interband transition and boost the plasmonic resonance along with silver. Then a planar plasmonic substrate is fabricated with an atomic MoS₂ layer on a silver surface. This MoS₂ monolayer prevents undesired molecules from penetrating and prevents interband transition. The existence of the MoS₂ layer in the silver film can potentially enhance surface plasmon resonance (SPR) sensitivity and stability. Moreover, a variety of materials, geometries, and their respective properties induce the formation of ohmic losses in surface plasmon propagation. Due to an increase in ohmic losses, the propagation length of surface plasmons becomes shorter, which restricts the electric field to penetrate deeper into the metal reducing the radiating properties. Thus, a novel bi-rhombic hybrid nanostrip waveguide has been modelled, as shown in Fig. 1, with two parallel rhombic layers utilizing a hybrid material of Ag with silicon ribbon to mitigate ohmic losses and enhance the propagation. The rhombic structure diminishes ohmic losses and the nanostrip waveguide strengthens the intensity of light in an optimal magnitude.

Furthermore, it is also necessary to reduce the side lobes for decreasing interference with components in an optical system thereby producing high plasmonic features, as well as obtaining high transmission and lowering power losses. Thus, a *graphite spherical resonator* is being used, where the spherical structure suppresses the side lobe because of the high efficiency, and thermal stability of

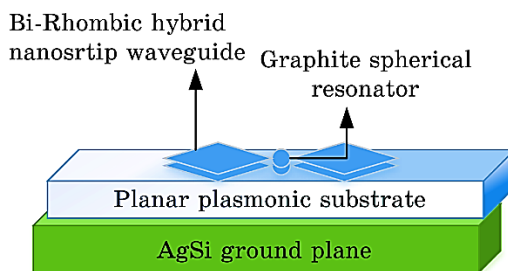


Fig. 1. Block diagram for nanoantenna design.

graphite and lowers the losses at optical frequencies, owing to the significant field confinement.

Thus, the proposed plasmonic nanoantenna mitigates losses and propagates the signal to a wide bandwidth and thereby increasing the nanoantenna radiation efficiency.

3.1. Design Specification of Proposed Nanoantenna

The proposed antenna consists of a resonator and waveguides 1 and 2 with a substrate. The nanoantenna was designed in HFSS with the following parameters to define the performance of the proposed plasmonic antenna. The resonator was designed with a radius of $r = 50$ nm; the waveguide 1 and 2 are designed symmetrically and identically with length and width of $L = 396$ nm and $W = 200$ nm, respectively. The angle between two adjacent sides of the rhombus is taken as $\Psi = 30^\circ$.

The complete visual of our proposed antenna is shown in Fig. 2. AgSi serves as a ground plane, where the silicon is coated with silver, which makes up the antenna. The atomic structure of MoS₂ is formed on the silver surface. Next, both parallel waveguides made of bi-rhombic hybrid nanostrips and a spherical resonator are employed. Our antenna model thus consists of an excitation field that is 10 nm in size and a feed line that is 12 nm (FL) in length and 10 nm in width (FW).

The substrate is designed with length, width, and thickness of $L = 900$ nm, $W = 500$ nm, and $T = 12$ nm, respectively. The air-gap thickness between adjacent layers is taken as $t_1 = 1$ nm and the air-gap from the substrate and waveguide and in-between the waveguides are taken as $t_2 = 0.2$ nm and $t_3 = 3$ nm, while substrate Ag and MoS₂ have the same characteristics: $L = 900$ nm, $W = 500$ nm, $T = 140$ nm, and $t_4 = 7$ nm.

For a working frequency of $\nu = 330$ THz ($\lambda = 909$ nm), the geometrical parameters for the antenna designs were optimized. Plas-

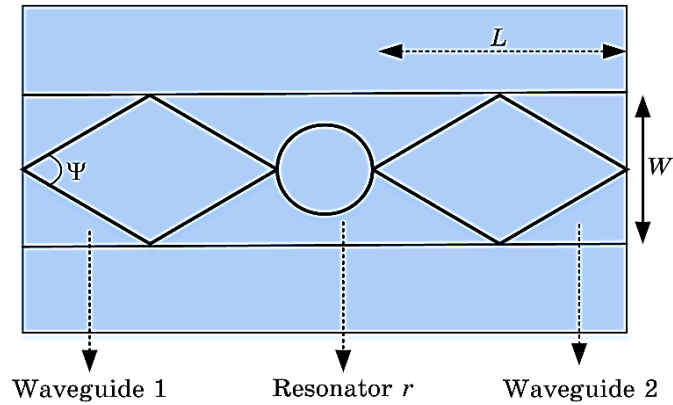


Fig. 2. Top view of the proposed antenna.

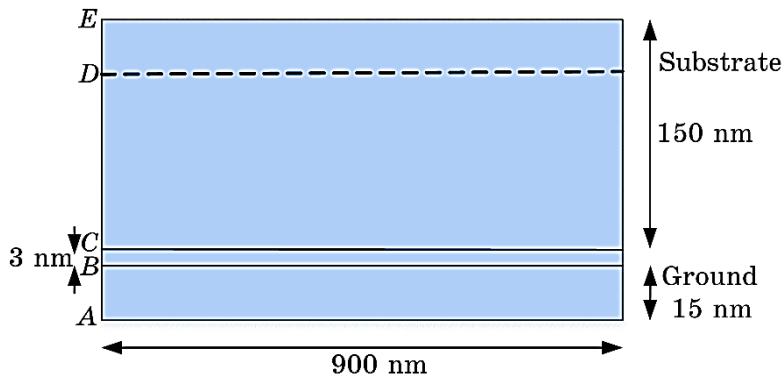


Fig. 3. Front view of the proposed antenna.

monic nanostructures were thought to be constructed of AgSi substrate with permittivity $\epsilon_r = 2.28$ and thickness $h = 150$ nm, all of which were considered as critical parameters. To mimic a ground plane, the substrate was terminated with an AgSi boundary condition, as seen in Fig. 3.

3.1.1. Plasmonic Material Integration

The AgSi material is a composite of silver and silicon, where the silver provides the high conductivity needed for the ground plane, and the silicon provides mechanical strength and thermal stability. The proposed method uses AgSi ground planes, which serve as the bottom layer of the antenna. The ground plane provides a low-impedance path for the return current, which is important for re-

ducing signal distortion and ensuring proper signal integrity. One advantage of using AgSi ground planes is that they offer low-loss performance at high frequencies, which is critical for nanoantenna. AgSi ground planes also have a high thermal conductivity, which can help dissipate heat generated.

Thus using AgSi ground planes for nanoantennas, creates a low-loss substrate material that supports the antenna structure while also minimizing any interference or scattering from the ground plane. AgSi is an excellent choice for this application because it provides a low-loss material with a high conductivity that can support the antenna structure.

Overall, the combination of low-loss performance, high thermal conductivity, mechanical stability, compatibility with fabrication techniques, and smooth surface makes AgSi ground planes an attractive choice for nanoantenna applications.

3.1.2. MoS₂ Monolayer

MoS₂ (molybdenum disulphide) is a two-dimensional material that has attracted significant attention in recent years due to its unique electronic and optical properties. MoS₂ layer is used as a planar plasmonic substrate in conjunction with silver surfaces to create a nanoantenna that can manipulate light at the nanoscale in this research.

Moreover, a MoS₂ layer is deposited on a silver surface; it can act as a dielectric spacer layer that enhances the plasmonic properties of the silver surface. Specifically, the MoS₂ layer can support surface plasmon polaritons (SPPs), which are collective oscillations of free electrons at the metal–dielectric interface. The SPPs can be excited by incident light, leading to enhanced electromagnetic fields and light–matter interactions at the interface. In addition, a major advantage of using a MoS₂ layer on a silver surface as a planar plasmonic substrate is that it can provide greater control over the plasmonic properties of the silver surface. By adjusting the thickness and dielectric properties of the MoS₂ layer, the frequency and intensity of the SPPs can be tuned, enabling the design of plasmonic devices with specific optical properties.

Additionally, MoS₂ layers are chemically stable and can withstand high temperatures, making them compatible with a range of fabrication techniques, including lithography and electron-beam deposition.

Overall, the use of MoS₂ layers on silver surfaces as planar plasmonic substrates offers a promising approach to designing and fabricating plasmonic devices with enhanced light–matter interactions at the nanoscale.

3.1.3. Novel Bi-Rhombic Hybrid Nanostrip Waveguide

The bi-rhombic shape of the waveguide allows for a more efficient coupling of light from the nanostrip into free space, which is important for applications such as nanoantennas. By using a bi-rhombic hybrid nanostrip waveguide as part of a nanoantenna, it is possible to achieve higher efficiency and stronger light–matter interactions.

The bi-rhombic shape of the waveguide can provide better confinement of light within the waveguide, resulting in higher intensity fields and stronger light–matter interactions. The bi-rhombic shape of the waveguide improves the coupling of light from the waveguide into free space, leading to more efficient light extraction and better radiation patterns. In addition, the bi-rhombic shape has specific resonant properties, allowing for precise control of the interaction between light and matter, where the resonance effects can be used to enhance absorption, scattering, or emission of light by nearby particles or molecules. Overall, the bi-rhombic structure serves as a versatile and effective tool for waveguides in nanoantennas, offering improved light confinement, and enhanced coupling to free space, tuneable resonant properties, and compatibility with nanoscale components.

The rhombic geometry allows, for more efficient utilization of the available space, enabling longer signal propagation paths. This extended path length results in reduced ohmic losses, as the electromagnetic fields experience less resistance along the transmission route. In addition, the rhombic geometry offers more degrees of freedom in design compared to traditional straight waveguides. This flexibility allows for better optimization of the waveguide parameters to match specific operational requirements. Furthermore, the geometry of the rhombic waveguide can be adapted to support multimode propagation, allowing for the transmission of multiple signals simultaneously. This can increase data throughput in communication systems.

3.1.4. Graphite Spherical Resonator

Numerous resonator geometries are being examined to seek dielectric resonators with desirable properties. It has been discovered that optimum geometries may have a broader bandwidth or superior linear polarisation properties. Due to the benefits and appealing qualities of a spherical resonator, such as their small weight, low cost, and very broad impedance bandwidth, the spherical resonator antennas have drawn more attention from antenna designers as a potential solution for inter/intra-chip wireless communication.

It is effective to employ graphene as a resonator for antennas because it allows for extreme miniaturization, homogeneous integration with graphene, effective dynamic tuning, and even transparency and mechanical flexibility. A potential material for the creation of miniature resonant THz antennas is graphene. Remarkably, even with straightforward geometries, strong direct matching to THz may be accomplished by utilizing a simple dipole-like plasmonic resonator. With the incredibly tiny electrical size and high radiation efficiency, the results are comparable.

4. RESULTS AND DISCUSSION

This research introduces a groundbreaking approach to enhance significantly antenna efficiency in inter/intra-chip optical wireless communication through the innovative utilization of plasmonic materials. A central challenge addressed in this work is the mitigation of interband transition phenomena, which often undermines overall performance. The proposed model unveils a unique and robust solution by introducing an AgSi ground plane composed of a silver-coated silicon cube. This incorporation of a silicon layer not only effectively counteracts interband transitions but also synergistically amplifies plasmonic resonance alongside silver. Moreover, the study meticulously designs and fabricates a planar plasmonic substrate, characterized by the strategic deposition of an atomic monolayer of MoS₂ onto a silver surface. This layer of MoS₂ plays a pivotal role as a defensive barrier, effectively thwarting unwanted molecule penetration and successfully suppressing interband transition effects. In the pursuit of practical implementation, the research pioneers a novel bi-rhombic hybrid nanostrip-waveguide configuration.

This innovative design integrates two parallel rhombic layers, ingeniously incorporating a hybrid material composition of silver and silicon ribbon. This arrangement is engineered to mitigate meticulously ohmic losses, thus significantly enhancing propagation efficiency. The geometric attributes of the rhombic layers decisively contribute to the reduction of ohmic losses, while the nanostrip waveguide component harmoniously intensifies light propagation to an optimal magnitude. The comprehensive nature of this research is exemplified through a rigorous series of experiments, simulated using ANSYS HFSS 2019 R3 software. Comparative analyses against conventional antenna models were exhaustively undertaken, unequivocally showcasing the superior performance achieved by the proposed antenna configuration. These robust experimental results decisively underscore the viability and practical significance of the proposed methodology in advancing the domain of inter/intra-chip optical wireless communication systems. For applications in optical

wireless nanolinks, the radiation characteristics of nanoantenna types are to be examined. To determine the associated directivity patterns, we employ a far-field boundary that is $\lambda/2\pi$ (≈ 100 nm) away from the nanoantenna.

4.1. Hypothesis

The hypothesis of this research is that the strategic integration of plasmonic materials and innovative structural designs can lead to a significant improvement in the efficiency of antennas for inter/intra-chip optical wireless communication. By utilizing plasmonic materials such as silver-coated silicon and MoS₂ combined with novel waveguide configurations, it is postulated that the interband transition issues and ohmic losses commonly encountered in such communication systems can be effectively mitigated. This, in turn, should result in enhanced antenna performance, opening new possibilities for more efficient and reliable optical wireless communication within and between the microchips.

4.2. Scientific Justification

The scientific justification for the proposed method lies in its synergistic integration of plasmonic material properties, barrier effects of MoS₂, advanced waveguide design, and rigorous simulation-based analysis. Through the careful consideration of these principles, the proposed method aims to mitigate known limitations and challenges, offering a comprehensive approach to improving antenna efficiency in optical wireless communication within the microchip environments.

4.3. Performance Analysis

The performance of the proposed antenna is analysed with various parameters and discussed in detail in the following section.

4.4. Electric Field

Figure 4 depicts the electric field of the antenna design for our proposed antenna design. The field depicts the physical area, which encircles electrically conducting particles and imposes power on all other energetic particles in the line of work, trying to attract them. Electric charges with different amplitudes are the sources of electric fields.

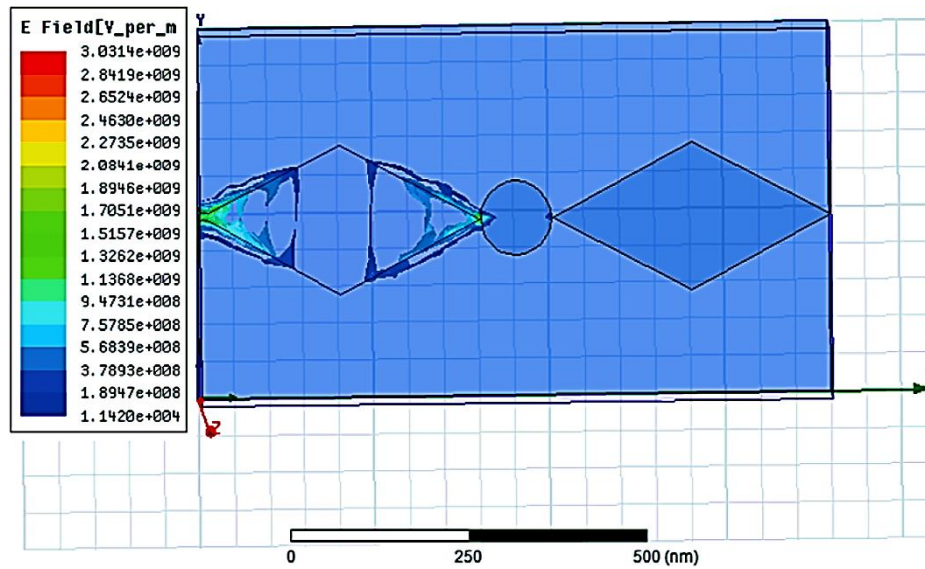


Fig. 4. E-field.

The electric field of a nanoantenna is obtained to be $9.4731 \cdot 10^9$ V/m that is strong enough to efficiently couple with the incident radiation and induce resonance in the antenna, but not so strong, that it may lead to material damage or excessive heating. In this research, the utilization of MoS_2 material with high permittivity enhances the electric field of the antenna; in addition, the plasmonic materials with high conductivity reduce the losses in the antenna and improve its performance.

4.4.1. Radiation Pattern

In general, high radiation efficiency is desirable for a nanoantenna to convert efficiently the input signal into radiated power. Radiation patterns are diagrammatic characterizations of the transmission of radiated energy into space as a function of manner. The optimum radiation efficiency of a nanoantenna depends on a variety of factors such as its size, shape, material properties, and the wavelength of the incident radiation. The radiation efficiency of a nanoantenna is defined as

$$\text{Radiation efficiency} = \frac{\text{The radiated power}}{\text{The output power}}.$$

Figure 5 depicts the patterns of radiation on the XYZ plane, and

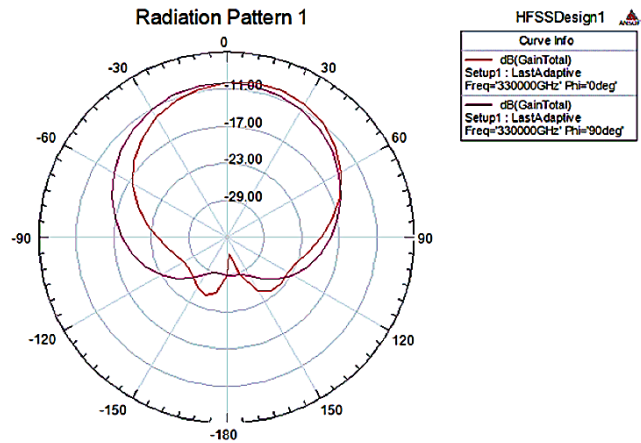


Fig. 5. Radiation pattern.

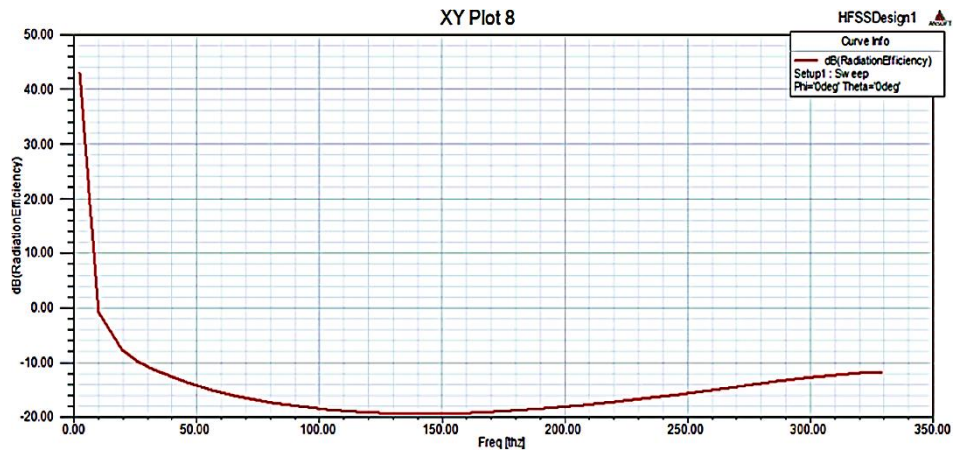


Fig. 6. Radiation efficiency.

the calculations were done with a working frequency of 330 THz and a wavelength of 909 nm. The proposed antenna violet colour depicts the magnetic gain field following a phase shift of 90 degrees, and its red colour represents the complete gain electric field at 0 degrees. To achieve high radiation efficiency, plasmonic materials are utilized in the design of nanoantennas, which enhanced the radiation efficiency by enabling strong coupling between the antenna and the incident radiation.

The radiation efficiency of our proposed model is shown in Fig. 6. With the X-axis in THz and the Y-axis in dB, the graph shows that the proposed antenna starts to have a gradual increase in effi-

ciency from 150 THz and achieves -11 dB at 329 THz, and then, we can also observe a steady increase in the radiation efficiency as the frequency approaches 350 THz.

4.4.2. Gain

The gain of a nanoantenna is a measure of its ability to convert input power into radiated power in a particular direction. The optimum gain of a nanoantenna would typically be the highest possible gain that can be achieved while meeting the other requirements, such as bandwidth, polarization, and radiation pattern.

The proposed approach gain is illustrated in Fig. 7, which shows a plotted 2D curve of gain value 9.3 dB at 329.6 THz of frequency. To achieve high gain in the proposed nanoantenna, several design techniques are used, such as increasing the antenna size, utilizing optimized bi-rhombic shape and structure, using high-permittivity materials, and employing better feeding and excitation with a resonator.

The 3D gain of our proposed method is depicted in Fig. 8. We achieved maximum gain using our method at 329 THz. It shows how the antenna radiates electromagnetic energy in different directions and can help visualize the directivity and gain of the antenna. The proposed high-gain antenna can improve signal quality and reduce interference, leading to better data rates and network performance. In sensing applications, high-gain antennas can improve the sensitivity and resolution of the system by focusing the radiation in

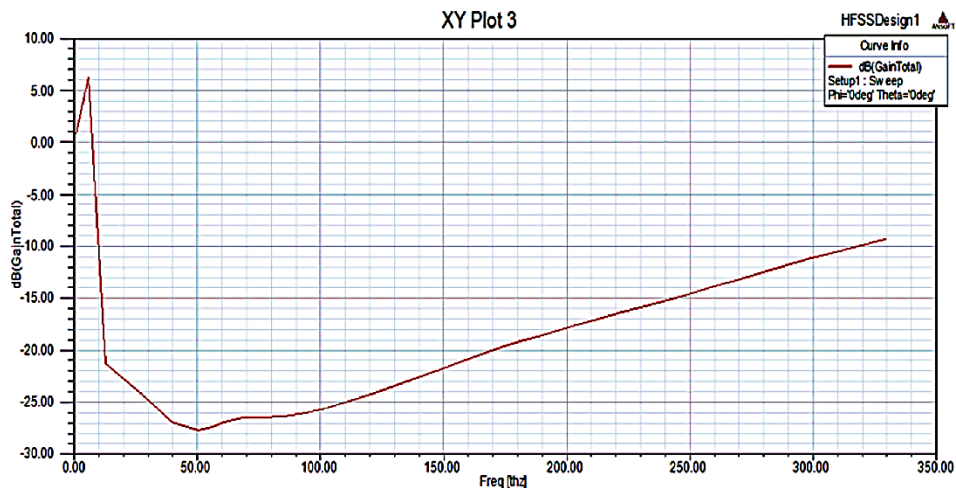


Fig. 7. 2D plot of gain.

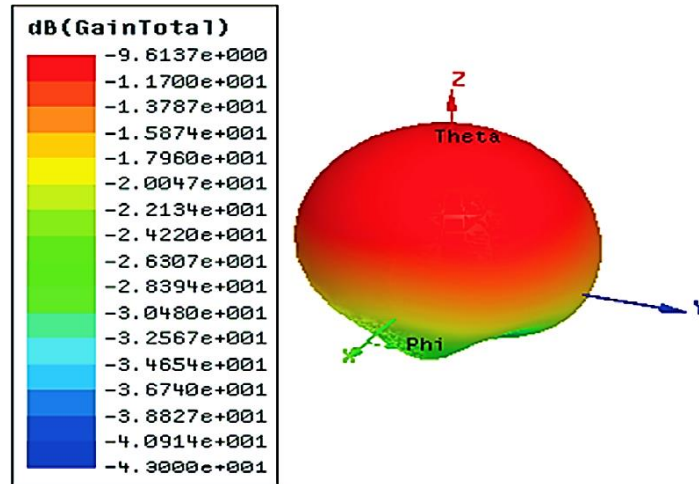


Fig. 8. 3D plot of gain.

a particular direction.

4.4.3. S-Parameters

S-parameters, or scattering parameters, are widely used in microwave and RF engineering to characterize the behaviour of linear electrical networks, such as antennas, amplifiers, and transmission lines. These parameters provide valuable insight into how energy is transmitted and reflected within the system. Understanding S-parameter curves from a physical perspective is essential for designing, analysing, and optimizing these systems. A typical S-parameter curve is represented on a complex plane, with the real part on one axis and the imaginary part on the other. The S-parameters of a nanoantenna refer to the scattering parameters or the reflection and transmission coefficients of the antenna. The S-parameters describe how electromagnetic waves are scattered or transmitted by the antenna, when it is excited by an incident wave.

In Figure 9, the S-parameter for our method is shown, which refers to the reflection coefficient of the antenna, which measures the amount of energy that is reflected from the antenna, when it is excited by an incident wave.

Frequency is considered from 0 to 350 THz, while S_{11} of about -7.56 dB is obtained, which shows low reflection loss. A low reflection coefficient (S_{11}) indicates that a small portion of the incident energy is reflected from the antenna, while the majority of the energy is transmitted or absorbed by the antenna.



Fig. 9. S-parameter.

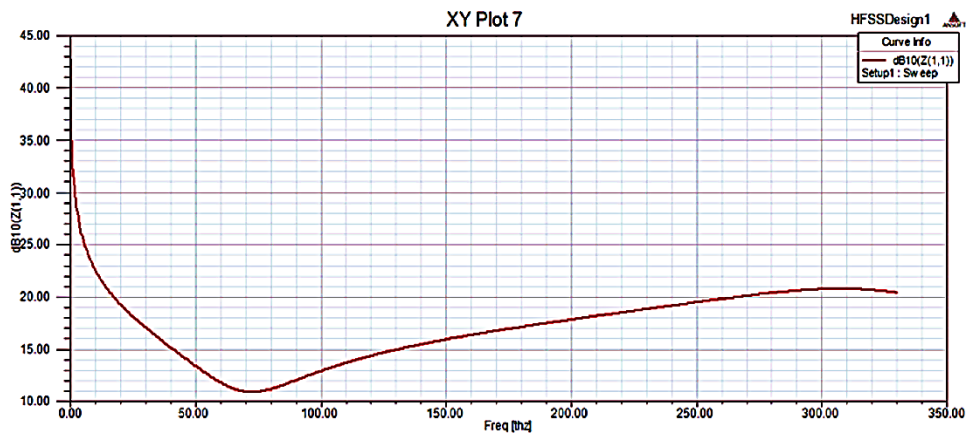


Fig. 10. Z-parameter.

4.4.4. Z-Parameter

The Z-parameters of a nanoantenna refer to a set of four complex-valued parameters that describe the input-output relationship of the antenna in terms of its impedance properties. The Z-parameters of a nanoantenna are important for understanding how the antenna interacts with the electromagnetic fields of the surrounding environment, and for optimizing the performance of the antenna.

Figure 10 shows the Z-parameter of our proposed antenna model. The frequency was considered optimum between 0 to 350 THz and the Z_{11} was found to be minimal with 11.49 dB at 70 THz and raised to 21.03 dB at 300 THz. Thus, the obtained Z-parameters

show a better impedance matching of the antenna to the source with the proposed plasmonic material. Thereby ensuring efficient energy transfer and minimized reflections, which are important for optimizing the antenna performance in a real-world application.

4.4.5. Accepted Power

A nanoantenna is designed to operate in the optical region of the electromagnetic spectrum, where the incident radiation has a high energy density. As a result, the power that can be absorbed by the antenna should be quite high, typically on the order of microwatts to milliwatts. The accepted power in a nanoantenna refers to the maximum power that the antenna can handle without damage, and it depends on several factors, including the material properties and geometry of the antenna, the frequency of operation, and the environmental conditions.

Our proposed-method accepted power is shown in Fig. 11. The graph describes that at the frequency of 330 THz, the accepted power seems to be of 0.80 V/m. This shows that the optimum accepted power of a nanoantenna establishes a trade-off between maximizing the efficiency of energy conversion and minimizing the risk of damage to the antenna or the surrounding environment.

4.5. Comparative Analysis

A comparative analysis of radiation efficiency vs frequency of a nanoantenna for varying angle can be useful in understanding how



Fig. 11. Accepted power.

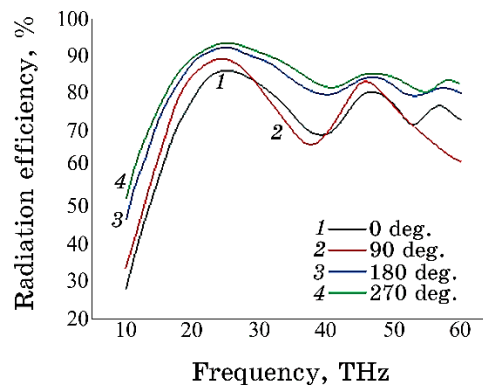


Fig. 12. Comparison of radiation efficiency with varying angles of antenna.

the performance of the antenna changes with respect to the angle of incidence and the operating frequency. The radiation efficiency was compared with a frequency of 10 to 60 THz for various angles of rotation (\varnothing) as shown in Fig. 12. The graph was plotted with the values obtained from HFSS analysis. The graph depicts that the optimum radiation efficiency is obtained in 180° . When the angle of incidence changes, the radiation pattern of the antenna also changes that affects the radiation efficiency. At the same time, the operating frequency of the antenna also affects the radiation efficiency, as the antenna dimensions and shape are optimized for a specific frequency range.

The impedance of an antenna is a measure of the opposition to the flow of current in the antenna, and it affects the efficiency of power transfer between the antenna and the source or load. The impedance of the proposed method is compared with the frequency of 10 to 35 THz for different angles of an antenna as shown in Fig. 13. The graph clearly shows that as the angle increases, the impedance related to frequency also increases. The results of the analysis provide insights into the optimal angle and frequency range for the antenna to achieve matching impedance with the source or load, which maximizes the power transfer efficiency.

The results of the comparative analysis between electric field and varying angle provides insights into the optimal angle and frequency range for the antenna to achieve a strong and directional electric field, which maximizes the radiation efficiency and the signal strength. The electric field based on the varying angle with frequency ranging from 10 to 60 THz is examined and the graph has been plotted. Figure 14 shows that the angle deviation generally reduces the electric field. The graph depicts a minimum of 250 V/m of electric field even at maximum angle variation.

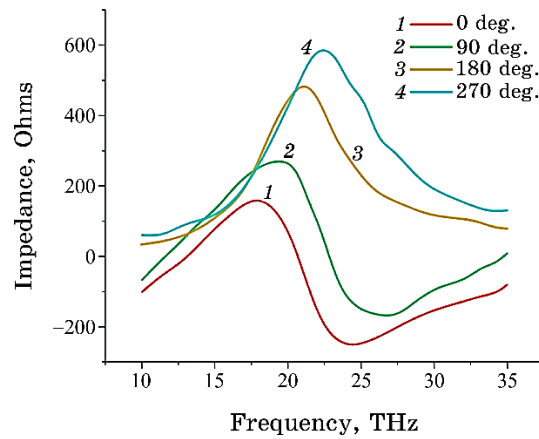


Fig. 13. Comparison of impedance with varying angles of antenna.

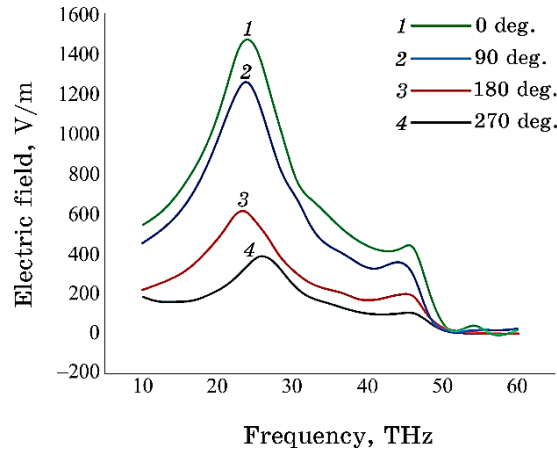


Fig. 14. Comparison of an electric field with varying angles of antenna.

The S_{11} parameter of the proposed method is compared with DRA (Spherical Dielectric Radiation Antenna) [22].

Figure 15 depicts that the reflection of an antenna is minimum between the frequencies of 440 to 560 THz. The proposed nanoantenna has a lower S_{11} parameter than the conventional antenna over a certain frequency range that indicates that the nanoantenna has a better impedance match and higher energy transfer efficiency in that range. Thus, the proposed antenna is superior to the conventional design based on the S_{11} parameter and has the potential to provide better performance than conventional antennas due to their smaller size, higher radiation efficiency, and unique properties, such as plasmonic resonance.

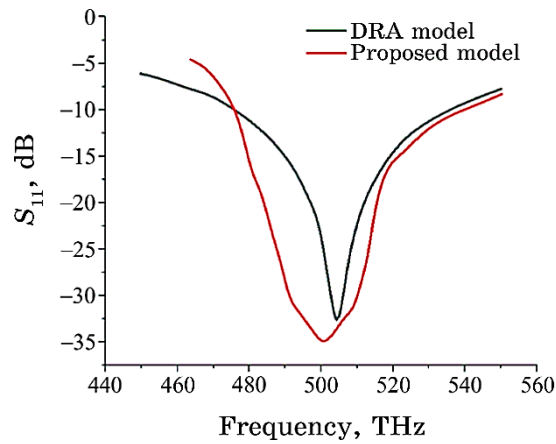


Fig. 15. Comparison of the S_{11} parameter of the proposed antenna.

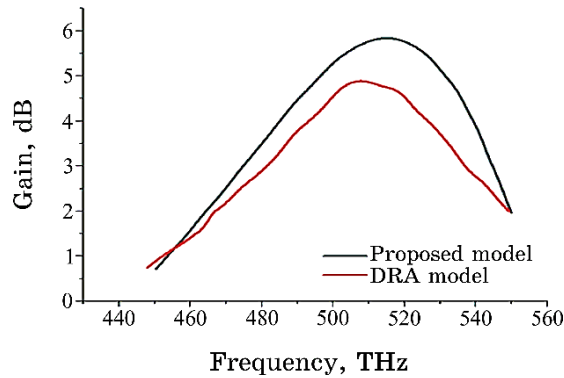


Fig. 16. Comparison of gain of the proposed antenna.

The above graph depicts that the proposed antenna gain is higher than the DRA (Spherical Dielectric Radiation Antenna) as shown in Fig. 16.

The proposed nanoantenna has a higher gain than the conventional antenna in a certain frequency, it indicates that the nanoantenna can radiate more energy within the frequency and is more effective at directing the energy of the signal. This shows that the proposed antenna have the potential to provide higher gain than conventional antennas due to their smaller size and ability to generate and control surface plasmons. Thus, when compared to the conventional one and thereby, the applicability of the proposed antenna is higher. However, while simulations demonstrate improved performance, real-world results might deviate due to factors such as manufacturing tolerances, non-ideal material behaviours, and fabri-

cation limitations. The study may not account for all possible external influences and interactions that the antenna system might experience in dynamic operational environments.

5. CONCLUSION

The robust plasmonic nanoantenna design for intra/inter-chip optical wireless communication has been proposed and mathematically demonstrated with ANSYS HFSS simulation, which operates at a frequency of 330 THz and is intended for 6G applications. Our proposed approach is very effective in communicating successfully the data without significant losses and propagating the signal to a wide bandwidth, hence enhancing the nanoantenna radiation efficiency. Our model results in an increased gain, efficiency, transmission coefficients, impedance properties, and accepted power. The proposed antenna also outperformed the conventional techniques with an increase in efficiency of 11.57 dB and a gain of 9.3 dB, thus, proving the applicability of the proposed plasmonic antenna design in 6G inter/intra-chip optical wireless communications. The future of chip-level optical wireless communication lies in advancing robust plasmonic nanoantenna designs for both inter and intra-chip communication. These innovations promise ultra-high-speed data transfer within the integrated circuits, enhancing performance and enabling the next era of efficient and compact computing systems.

REFERENCES

1. D. G. Baranov, D. A. Zuev, S. I. Lepeshov, O. V. Kotov, A. E. Krasnok, A. B. Evlyukhin, and B. N. Chichkov, *Optica*, **4**, Iss. 7: 814 (2017); <https://doi.org/10.1364/OPTICA.4.000814>
2. S. Eslami and S. Palomba, *Nano Convergence*, **8**: Article No. 41-1 (2021); <https://doi.org/10.1186/s40580-021-00290-7>
3. E. Corcione, D. Pfezer, M. Hentschel, H. Giessen, and C. Tarin, *Sensors*, **22**, No. 1: 7 (2021); <https://doi.org/10.3390/s22010007>
4. Sreejyothi Sankararaman, Krishna Balasubramanian, and Revathy Padmanabhan, *Conference on Lasers and Electro-Optics (9–14 May 2021, San Jose, California, United States)*. *OSA Technical Digest* (Eds. J. Kang, S. Tomasulo, I. Ilev, D. Müller, N. Litchinitser, S. Polyakov, V. Podolskiy, J. Nunn, C. Dorrer, T. Fortier, Q. Gan, and C. Saraceno) (Optica Publishing Group: 2021), paper JW1A.183; https://doi.org/10.1364/CLEO_AT.2021.JW1A.183
5. Mohammad Javad Rabienejhad, Azardokht Mazaheri, and Mahdi Davoudi-Darareh, *Chin. Phys. B*, **30**, No. 4: 048401 (2021); [doi:10.1088/1674-1056/abd38e](https://doi.org/10.1088/1674-1056/abd38e)
6. Sergi Abadal, Chong Han, and Josep Miquel Jornet, *IEEE Access*, **8**, No. 12: 278 (2019); [doi:10.1109/ACCESS.2019.2961849](https://doi.org/10.1109/ACCESS.2019.2961849)

7. O. M. Haraz, M. M. M. Ali, and T. A. Denidni, *2021 IEEE 19th International Symposium on Antenna Technology and Applied Electromagnetics (ANTEM-2012)* (Winnipeg, Canada: IEEE Canada: 2021), p. 1.
8. Giovanna Calò, Gaetano Bellanca, Marina Barbiroli, Franco Fuschini, Giovanni Serafino, Davide Bertozzi, Velio Tralli, and Vincenzo Petruzzelli, *Optics Express*, **29**, No. 20: 31212 (2021); <https://doi.org/10.1364/OE.427633>
9. Demos Serghiou, Mohsen Khalily, Tim W. C. Brown, and Rahim Tafazolli, *IEEE Communications Surveys & Tutorials*, **24**, Iss. 4: 1957 (2022); [doi:10.1109/COMST.2022.3205505](https://doi.org/10.1109/COMST.2022.3205505)
10. Nitin Gupta and Anuj Dhawan, *OSA Continuum*, **4**, No. 11: 2970 (2021); [doi:10.1364/OSAC.430824](https://doi.org/10.1364/OSAC.430824)
11. Fei Dai, Yawen Chen, Haibo Zhang, and Zhiyi Huang, *arXiv:2109.14878*; <https://doi.org/10.48550/arXiv.2109.14878>
12. Shuchi Tripathi, Nithin V. Sabu, Abhishek K. Gupta, and Harpreet S. Dhillon, *arXiv:2102.10267*; <https://doi.org/10.48550/arXiv.2102.10267>
13. Arjun Singh, Michael Andreello, Ngwe Thawdar, and Josep Miquel Jornet, *IEEE Journal on Selected Areas in Communications*, **38**, No. 9: 2104 (2020); <https://doi.org/10.1109/JSAC.2020.3000881>
14. Bin Zhang, Josep M. Jornet, Ian F. Akyildiz, and Zhi P. Wu, *IEEE Access*, **7**: 33214 (2019); <https://doi.org/10.1109/ACCESS.2019.2903493>
15. Evgenia Rusak, Jakob Straubel, Piotr Gładysz, Mirko Göddel, Andrzej Kędziorowski, Michael Kühn, Florian Weigend, Carsten Rockstuhl, and Karolina Slowik, *Nature Communications*, **10**: Article No. 5775-1 (2019); <https://doi.org/10.1038/s41467-019-13748-4>
16. Mona Nafari and Josep Miquel Jornet, *IEEE Access*, **5**: 6389 (2017); <https://doi.org/10.1109/ACCESS.2017.2690990>
17. A. A. C. Alves, M. C. Melo, J. J. Siqueira, F. Zanella, J. R. Mejia-Salazar, and C. S. Arismar, *2020 2nd 6G Wireless Summit (6G SUMMIT) (8-11 June, 2021, Porto, Portugal)*, p. 1.
18. Inzamam Ahmad, Shakir Ullah, Jalal ud din, Sadiq Ullah, Waseem Ullah, Usman Habib, Salahuddin Khan, and Jaume Anguera, *Applied Sciences*, **11**, No. 19: 8893 (2021); <https://doi.org/10.3390/app11198893>
19. Richard Victor Biswas and Farhadur Arin, *Research Square*, **12**: 1 (2021); <https://doi.org/10.21203/rs.3.rs-1079661/v1>
20. Sasmita Dash, Goutam Soni, Amalendu Patnaik, Christos Liaskos, Andreas Pitsillides, and Ian F. Akyildiz, *Plasmonics*, **16**, No. 5: 1855 (2021); <https://doi.org/10.1007/s11468-021-01449-y>
21. S. Kavitha, K. V. S. S. S. Sairam, and Ashish Singh, *SN Applied Sciences*, **4**: Article No. 114-1 (2022); <https://doi.org/10.1007/s42452-022-04986-1>
22. Rajveer S. Yaduvanshi, Rama Krishna Yadav, Saurabh Katiyar, Suresh Kumar, and Harish Parthasarathy, *Frequenz*, **75**, Nos. 1-2: 49 (2021); <https://doi.org/10.1515/freq-2020-0086>